Behavioral/Systems/Cognitive

Bidirectional Synaptic Plasticity and Spatial Memory Flexibility Require Ca^{2+}-Stimulated Adenylyl Cyclases

Ming Zhang,[1] **Daniel R. Storm,**[2] **and Hongbing Wang**[1]

[1]Department of Physiology, Neuroscience Program, Michigan State University, East Lansing, Michigan 48824, and [2]Department of Pharmacology, University of Washington, Seattle, Washington 98195

When certain memory becomes obsolete, effective suppression of the previously established memory is essential for animals to adapt to the changing environment. At the cellular level, reversal of synaptic potentiation may be important for neurons to acquire new information and to prevent synaptic saturation. Here, we investigated the function of Ca^{2+}-stimulated cAMP signaling in the regulation of bidirectional synaptic plasticity and spatial memory formation in double knock-out mice (DKO) lacking both type 1 and 8 adenylyl cyclases (ACs). In anesthetized animals, the DKO mutants showed defective long-term potentiation (LTP) after a single high-frequency stimulation (HFS) or two spaced HFSs at 100 Hz. However, DKO mice showed normal LTP after a single HFS at 200 Hz or two compressed HFSs at 100 Hz. Interestingly, reversal of synaptic potentiation as well as *de novo* synaptic depression was impaired in DKO mice. In the Morris water maze, DKO mice showed defective acquisition and memory retention, although the deficits could be attenuated by overtraining or compressed trainings with a shorter intertrial interval. In the reversal platform test, DKO animals were impaired in both relearning and old memory suppression. Furthermore, the extinction of the old spatial memory was not efficient in DKO mice. These data demonstrate that Ca^{2+}-stimulated AC activity is important not only for LTP and spatial memory formation but also for the suppression of both previously established synaptic potentiation and old spatial memory.

Introduction

Memory formation consists of mechanistically different phases. The efficient acquisition of information as well as consolidation normally requires activity-dependent synaptic modifications. Another important aspect of memory process is that, when certain memory becomes obsolete, effective suppression of the previously established memory may be essential for behavioral adaptations (Bouton, 2004; Myers et al., 2006). Theoretically, the bidirectional regulation of synaptic strength may be functionally involved in the dynamic behavioral changes during different stages of memory processes (Braunewell and Manahan-Vaughan, 2001; Huang and Hsu, 2001; Silva, 2003; Diamond et al., 2005).

Previous studies with different animal models have demonstrated an important role of cAMP signaling in regulating synaptic plasticity and memory formation (Nguyen and Woo, 2003; Abel and Nguyen, 2008; Lee et al., 2008). Because Ca^{2+}-stimulated adenylyl cyclases (ACs) couple the activity-dependent increase of intracellular Ca^{2+} to cAMP elevation, their function in regulating synaptic modification and memory formation has been suggested. Of all the identified ACs, type 1 and type 8 ACs (AC1 and AC8) are the major Ca^{2+}-stimulated ACs in the CNS (for review, see Wang and Storm, 2003). Previous studies have demonstrated that the activation of certain cAMP-regulated signaling molecules during long-term potentiation (LTP) and long-term memory formation requires AC1 and AC8 activity (Sindreu et al., 2007; Eckel-Mahan et al., 2008; Wieczorek et al., 2010). Double knock-out (DKO) mice lacking both AC1 and AC8 do not show Ca^{2+}-stimulated elevation of cAMP *in vitro* (Wong et al., 1999). Functionally, DKO mice are impaired for late-phase LTP *in vitro* and show defective long-term retention of contextual memory. Furthermore, enhancement of Ca^{2+}-stimulated AC activity facilitates LTP, the maintenance of remote fear memory, and the activation of certain plasticity-related signaling transduction (Wang et al., 2004; Shan et al., 2008). However, although the bidirectional modification of both synaptic changes and memory process is essential for normal brain function, little is known about how Ca^{2+}-stimulated cAMP signaling regulates synaptic remodification and memory flexibility (such as relearning and old memory suppression).

In the present study, we first examined how disruption of Ca^{2+}-stimulated AC in DKO mice affected LTP, long-term depression (LTD), and suppression of synaptic potentiation (i.e., depotentiation) at the Schaffer collateral–CA1 synapses in the hippocampus. To examine these activity-dependent bidirectional synaptic modifications without significant disruption of the intact neuronal circuit, we performed electrophysiology *in vivo* with anesthetized animals. Next, we used different Morris water maze paradigms to examine *de novo* spatial learning, suppression of old spatial memory along with relearning a new platform location, and memory extinction in DKO mice. Our data suggest novel functions of Ca^{2+}-stimulated cAMP signaling in synaptic and memory flexibility.

Received Dec. 29, 2010; revised May 10, 2011; accepted May 30, 2011.

Author contributions: M.Z., D.R.S., and H.W. designed research; M.Z. performed research; M.Z. and H.W. analyzed data; M.Z. and H.W. wrote the paper.

This work was supported by NIH Grants MH076906 (H.W.) and MH073601 (D.R.S.).

Correspondence should be addressed to Hongbing Wang at the above address. E-mail: wangho@msu.edu.

DOI:10.1523/JNEUROSCI.0009-11.2011

 0270-6474/11/3110174-10$15.00/0

Materials and Methods

Animals. DKO mice for type 1 and type 8 adenylyl cyclases (AC1 and AC8) were previously reported (Wong et al., 1999). They were backcrossed to C57BL/6 background for at least 12 generations. Young adult (10- to 15-week-old) male DKO and wild-type (WT) control mice with body weight of 20–27 g were used in electrophysiological and behavioral studies. All animals were kept in the University Laboratory Animal Resources facility with 12 h light/dark cycle and had *ad libitum* access to food and water. All manipulations were in compliance with the guidelines of Institutional Animal Care and Use Committee at Michigan State University.

In vivo *electrophysiological recordings at Schaffer collateral–CA1 synapses.* Mouse was deeply anesthetized with Nembutal sodium solution (Ovation) at a dose of 100 mg/kg (intraperitoneally) within its home cage, and then mounted to a stereotaxic frame (David Kopf Instruments). The anal temperature of mouse was monitored and kept at 37.0 ± 0.5°C by placing the mouse on a Physitemp Controller-connected heating pad. Medical oxygen with 5% CO_2 was continuously supplied through a tube put in front of the mouse snout. Two electrodes (a pair of 100 μm outer diameter Teflon-coated wires; WPI) were slowly inserted into the brain through drilled holes. Stimulating electrode was placed at Schaffer collaterals of dorsal hippocampus (AP, −1.7–1.9 mm; ML, 1.7–1.9 mm; DV, 1.6–2.0 mm from skull surface), and recording electrode was placed at the ipsilateral striatum radiatum of hippocampal CA1 area (AP, −1.7–1.9 mm; ML, 1.2–1.3 mm; DV, 1.5–1.9 mm). Placements of the two electrodes were slowly adjusted to obtain optimal response of field EPSP (fEPSP). Electrophysiological signals were amplified and recorded by using a Powerlab System (ADInstruments). Stimulating pulses (100 μs duration) with an intensity that evoked one-half of maximum amplitude were delivered at 0.033 Hz to obtain a stable baseline for at least 30 min. Once a stable baseline was established, conditioning stimulations at the same intensity as used for baseline were delivered to induce LTP, LTD, or depotentiation. After induction, the sampling rate was returned to 0.033 Hz and recording lasted for at least 60 min. At the end of electrophysiological recordings, anode electrolytic current (0.4 mA, 2 s) was delivered to produce a thermolytic lesion at the tip of the electrode. Brains were fixed in 10% formalin, sliced by a vibratome, and then the location of the electrode tip was confirmed.

Input–output curve and paired-pulse facilitation. Single pulses with different stimulation intensities ranged from 25 to 300 μA were applied to achieve the input–output curve before baseline recording. Paired pulses with interpulse intervals from 20 to 500 ms (at the intensity that evoked 30% maximal amplitude) were applied to induce paired-pulse facilitation.

LTP induction. Two paradigms of tetanus stimulation were applied to induce LTP. The first paradigm was one train of 100 pulses at different stimulation frequencies (i.e., 50, 100, or 200 Hz). The second paradigm was two trains of 100 pulses at 100 Hz with either spaced (i.e., 5 min) or compressed (i.e., 1 min) intertetanus interval.

Depotentiation and LTD induction. For depotentiation studies, LTP was first induced by two high-frequency stimulation (HFS) trains (100 pulses at 100 Hz for each train) with 1 min intertetanus interval. Then, low-frequency stimulation (LFS) consisting of 900 pulses at 1 Hz was delivered 5 min after the second HFS. For the induction of *de novo* synaptic depression, LFS consisting of 900 pulses at 1 Hz was delivered to naive Schaffer collateral–CA1 synapses after a stable baseline was established.

Morris water maze training. The training apparatus was a circular pool (125 cm in diameter) filled with clean water (19–20°C) and covered with white polypropylene beads (generous gifts from local Quality Dairy bottling facility). A circular platform (9 cm in diameter) was placed 1 cm below water surface. All animal activities were automatically recorded and measured by a video-based Morris water maze tracking system (WaterMaze; Coulbourn Instruments). Most of the water maze experiments consisted of three training phases: cued-platform (i.e., visible platform) training, the initial hidden platform training, and the reversal hidden platform training. For each training trial, a mouse was allowed to sit on the platform for 20 s after climbing onto the platform, or being manually guided to the platform if the maximal trial duration of 90 s had elapsed. In the cued-platform training, a small red flag (2 × 2 cm), which stood 5 cm above water surface, was attached to the platform. Locations of this cued platform were randomly altered for each trial. Mice were trained four trials per day with intertrial interval (ITI) of 20–30 min. In general, all mice were able to find the cued platform with <20 s after 2 d of training. For the later training stages, the red flag was removed from the platform, and the platform was placed at a new location that had never been used during the cued-platform trainings. Extra-maze cues (e.g., two wall posters) were presented as spatial references during the hidden platform trainings.

In water maze experiment 1 (WME-1), mice were first trained to find the cued/visible platform, and then trained by two trials per day with ITI of 4 h from day 1 to 6 for the initial hidden platform training stage. On day 7, the animals were subjected to a probe test, during which the platform was removed from the pool and mouse was released from the opposite quadrant of the initial platform location. The duration of the probe test was 60 s, after which the mouse was guided to the initial platform location and allowed to sit on the experimenter's hand for 20 s to minimize the impact of probe test on the performance of the subsequent training sessions. Then, mice were further trained for additional 6 d (from day 8 to day 13) for the same platform location by using the same training protocol as that from day 1 to 6. On day 14, the animals were subjected to a second probe test. During the reversal hidden platform training stage, the platform was moved to the opposite quadrant. By using the same training strategy (i.e., two trials per day with ITI of 4 h), mice were trained to find the new platform location for 4 d. A probe test was performed 24 h after the fourth day of reversal training. An additional 4 d of reversal training was performed and followed by another probe test 24 h after the last reversal training session. A schematic illustration for WME-1 is presented in Figure 4*A*.

In water maze experiment 2 (WME-2), mice were first pretrained to find the visible platform as described above. Second, the animals were trained to find the hidden platform by four trials per day with ITI of 30 min. A probe test was performed on day 7. The animals were further trained to find the hidden platform for additional 3 d. Twenty-four hours after the last hidden platform training, two extinction trials were performed each day with ITI of 4 h for 3 d. During each extinction trial, mouse was released from the opposite quadrant and allowed to swim for 60 s in the pool with the platform removed. At the end of each trial, mouse was immediately picked up and returned to its home cage. The time that mouse spent in the target quadrant as well as the crossing number over the platform location were recorded. A schematic illustration for the WME-2 is presented in Figure 6*A*.

In water maze experiment 3 (WME-3), we examined whether the visible platform pretraining experience influences spatial memory formation. Naive WT and DKO mice, without any visible platform training, were trained to locate the hidden platform by four trials each day with ITI of 30 min for 6 d. The first probe test was performed on day 7. The animals were further trained for 3 more days (i.e., from day 8 to 10). The second probe test was performed on day 11.

In water maze experiment 4 (WME-4), another two groups of naive WT and DKO mice were first pretrained to find the cued/visible platform. Then, they were examined by hidden platform training. The procedure of hidden platform training was essentially the same as that of WME-3, except that ITI of 1 min was used.

Data analysis. Changes of fEPSP initial slope following conditioning stimulus were expressed as percentage to that of baseline values. The average of fEPSPs collected in every 2 min was used for data presentation. Establishment of LTP/LTD was confirmed by comparing the fEPSP slopes at 50–60 min after tetanus to the values of the fEPSP during the last 10 min of baseline recording. Repeated-measures ANOVA with time/quadrant/probe/stimulus intensity/paired-pulse interval as within-subject factors were used to analyze the electrophysiological and behavioral data. One- or two-way ANOVA was used to compare effects of multiple groups. *Post hoc* Duncan tests were applied between groups, and pairwise least significant difference (LSD) tests were applied within groups when appropriate. Unpaired Student's *t* test was used to compare

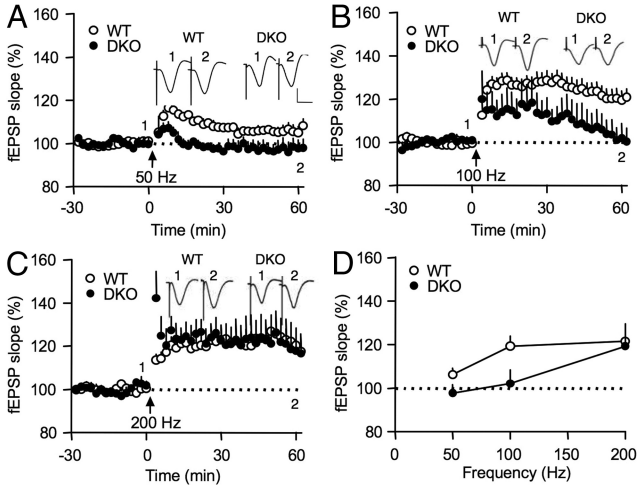

Figure 1. Frequency-dependent induction of long-term potentiation at the Schaffer collateral–CA1 synapses in DKO mice. ***A***, Tetanus stimulation with one train of 100 pulses at 50 Hz was ineffective to induce LTP in both WT ($n = 5$) and DKO groups ($n = 5$). ***B***, Tetanus stimulation with one train of 100 pulses at 100 Hz was sufficient to induce LTP in WT ($n = 9$) but not in DKO mutant mice ($n = 6$). ***C***, Tetanus stimulation with one train of 100 pulses at 200 Hz was sufficient to induce LTP in both groups ($n = 5$ for WT; $n = 5$ for DKO). ***D***, The frequency–response function curve was right-shifted in DKO mutants when compared with WT controls. The arrows indicate the delivery of tetanus stimulation. The insets are representative fEPSP traces taken before and after tetanus stimulation at the indicated time points. Calibration: 10 ms, 1 mV.

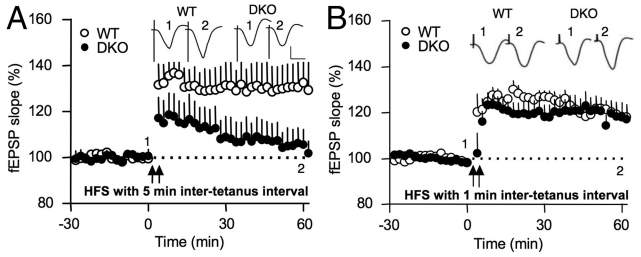

Figure 2. Induction of LTP in DKO mutants by two high-frequency stimulations with spaced or compressed intertetanus interval. ***A***, WT ($n = 6$) but not DKO mice ($n = 7$) showed robust LTP after two trains of HFS (100 Hz) delivered 5 min apart. ***B***, Both groups ($n = 7$ for each group) showed significant LTP after two trains of HFS (100 Hz) delivered 1 min apart. The arrows indicate the delivery of tetanus stimulations. The insets are representative fEPSP traces taken before and after tetanus stimulation at the indicated time points. Calibration: 10 ms, 1 mV.

two independent groups. All data were expressed as average ± SE and considered to be statistically significant if $p < 0.05$ was reached.

Results

Induction of LTP in DKO mutants by one train of HFS with different frequencies

Previous studies have demonstrated that Ca^{2+}-stimulated AC activity is required for LTP *in vitro* by using acute hippocampal slices (Wong et al., 1999). To examine how LTP is regulated *in vivo* with undisrupted neuronal network, we examined fEPSPs at the Schaffer collateral–CA1 synapses with anesthetized young adult mice. After a stable baseline recording was established, we first used one train of 100 pulses at different frequencies to induce LTP. Delivery of HFS at 50 Hz failed to induce LTP in both WT and DKO mice (all $p > 0.05$, two-way ANOVA with repeated measures). WT mice showed mild but not significant fEPSP potentiation (106.2 ± 2.9%) at 50–60 min after HFS. The change of fEPSP was 97.7 ± 3.9% for DKO animals (Fig. 1*A*). After delivering HFS at 100 Hz, WT mice showed significant LTP (120.2 ± 4.1%; $p < 0.01$ when compared with baseline). In contrast, DKO mutants did not show LTP (102.1 ± 6.3%; $p > 0.6$ when compared with baseline). The fEPSP slope changes induced with one train HFS at 100 Hz were significantly different between WT and DKO animals (genotype: $F_{(1,13)} = 6.0$, $p < 0.05$; genotype by time interaction: $F_{(9,117)} = 4.7$, $p < 0.0001$) (Fig. 1*B*). When tetanus frequency was increased to 200 Hz, both groups showed robust LTP (121.5 ± 8.0% for WT, and 119.2 ± 7.3% for DKO; both $p < 0.05$ when compared with baseline fEPSPs), and the LTP were comparable between the two groups ($p > 0.9$) (Fig. 1*C*).

As shown in Figure 1*D*, the frequency–response function curve is right-shifted in DKO mutants when compared with WT controls. Two-way ANOVA indicated that there were significant main effects of genotype ($F_{(1,29)} = 4.3$; $p < 0.05$) and HFS frequency ($F_{(1,29)} = 4.7$; $p < 0.05$) on the frequency–response curve, suggesting that Ca^{2+}-stimulated ACs might be involved in the regulation of the stimulation threshold for LTP induction.

LTP induction in DKO mutants by HFS with spaced or compressed intertetanus interval

Because stronger stimulation may be required to induce LTP in DKO animals, we further tested whether multiple trains of HFS at 100 Hz would be sufficient for the induction of LTP in DKO mutants. First, we delivered two trains of 100 pulses at 100 Hz with an intertetanus interval of 5 min, which was referred to as spaced HFS stimulation in two previous studies (Woo et al., 2003; Kim et al., 2010). WT mice showed significant LTP (130.7 ± 10.7%; $p < 0.05$ when compared with baseline), while DKO mutants failed to show LTP (104.8 ± 6.5%; $p > 0.3$ when compared with baseline) (Fig. 2*A*). The difference between WT and DKO animals for fEPSP changes was significant ($F_{(1,11)} = 4.9$; $p < 0.05$).

Next, we used two trains of 100 pulses with a more compressed intertetanus interval (i.e., 1 min compared with the spaced HFS stimulation with intertetanus interval of 5 min) to induce LTP. Interestingly, this protocol successfully resulted in significant LTP in both groups. WT animals showed 119.3 ± 4.3% potentiation, and DKO animals showed 117.5 ± 5.6% potentiation ($p < 0.05$ for both WT and DKO animals when compared with the baseline fEPSP values). Furthermore, there was no significant difference between the two groups for fEPSP changes (genotype: $F_{(1,12)} = 0.1$, $p > 0.7$; genotype by time: $F_{(9,108)} = 0.3$, $p > 0.7$) (Fig. 2*B*). These results demonstrate that increasing stimulation strength with an optimal compressed intertetanus interval is sufficient to induce Ca^{2+}-stimulated ACs-independent LTP at an insufficient frequency (i.e., 100 Hz in this study). In addition to supporting that Ca^{2+}-stimulated cAMP signaling may regulate the threshold level of LTP induction, our data are also consistent with previous *in vitro* findings that protein kinase A (PKA) activity plays an important role for LTP induced by spaced rather than by compressed stimulation (Woo et al., 2003; Kim et al., 2010).

Ca^{2+}-stimulated AC regulates synaptic depression and depotentiation

Considering that the bidirectional synaptic changes (potentiation vs depression) might be differentially regulated by Ca^{2+}-stimulated cAMP signaling, we further examined whether the lack of AC1/AC8 could facilitate LTD in DKO mice. Consistent with several previous studies that show robust *in vivo* LTD induction with adult rodents (Heynen et al., 1996, 2000), we were able

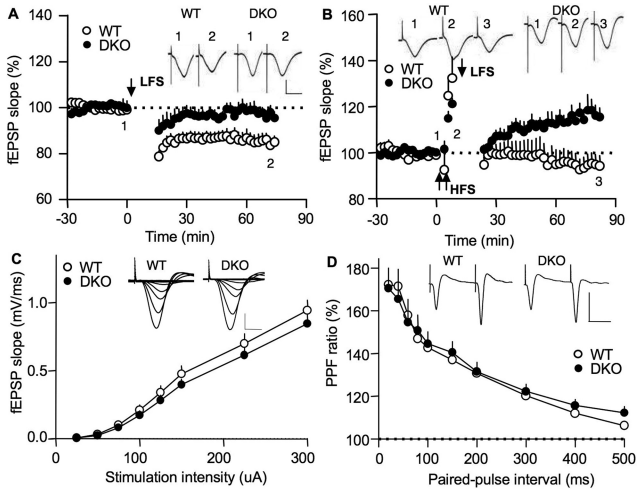

Figure 3. Both *de novo* synaptic depression and suppression of the previously established potentiation require Ca^{2+}-stimulated AC. ***A***, LFS of 900 pulses at 1 Hz induced LTD in anesthetized young adult WT ($n = 7$) but not in DKO mice ($n = 6$). The insets are representative fEPSP traces taken before and after LFS at the indicated time points. Calibration: 10 ms, 1 mV. ***B***, WT ($n = 7$) but not DKO ($n = 6$) mice showed obvious synaptic depotentiation, which was induced by LFS (900 pulses at 1 Hz) 5 min following the LTP stimulation protocol (2× HFS at 100 Hz with an intertetanus interval of 1 min). The insets are representative fEPSP traces taken at the indicated time. ***C***, The basal neural transmission was normal in DKO mice. Input–output curve was obtained by measuring fEPSP at different stimulation intensity. The insets are representative input–output traces. Calibration: 10 ms, 1 mV. ***D***, Paired-pulse facilitation was determined by paired stimulations with different interpulse intervals. The insets are representative traces with a paired-pulse interval of 80 ms. Calibration: 40 ms, 1 mV.

to induce significant *in vivo* LTD with 2- to 3-month-old mice by using the standard LFS induction protocol (i.e., 900 pulses at 1 Hz). As shown in Figure 3*A*, low-frequency stimulation with one train of 900 pulses at 1 Hz caused significant synaptic depression that lasted for at least 60 min in WT animals. The fEPSP decreased to 85.1 ± 2.8% of the baseline value ($p < 0.05$). However, DKO mutants failed to show LTD (96.7 ± 2.3%; $p > 0.1$ when compared with the baseline value). The group difference for fEPSP changes at 50–60 min after LFS was significant ($F_{(1,11)} = 10.1$; $p < 0.01$) between WT and DKO animals, indicating that LTD induction requires Ca^{2+}-stimulated AC activity *in vivo*.

Another important aspect of bidirectional synaptic modification is that the potentiated synapses could be suppressed or reversed (i.e., synaptic depotentiation). Because significant LTP can be stimulated by two trains of compressed HFS at 100 Hz with 1 min intertetanus interval in both groups, we used this HFS protocol followed by LFS (900 pulses at 1 Hz) to induce depotentiation. One hour after the LFS, the fEPSP in WT mice dropped to the baseline level (94.5 ± 4.5%; $p > 0.4$ compared with baseline before the HFS), indicating effective LFS-induced depotentiation. In contrast, there was no significant depotentiation in DKO mice, of which fEPSP remained potentiated at a level of 116.5 ± 4.6% to that of baseline value ($p < 0.001$ when compared with baseline) (Fig. 3*B*). Furthermore, there was a significant effect of genotype on fEPSP changes at 50–60 min after LFS ($F_{(1,11)} = 11.8$; $p < 0.01$).

Although the activity-dependent synaptic modification was severely impaired in DKO mice, these animals showed normal basal transmission and normal short-term plasticity. The data for input–output curve and paired-pulse facilitation were collected from mice used for LTP, LTD, and depotentiation studies. We found no significant genotype effects for the pooled input–output curve (genotype: $F_{(1,70)} = 0.9$, $p = 0.3$; genotype by stimulus intensity: $F_{(7,490)} = 0.8$, $p = 0.6$; $n = 38$ for WT; $n = 34$ for DKO) (Fig. 3*C*). There was also no significant difference for paired-pulse facilitation between the two groups (genotype: $F_{(1,57)} = 0.03$, $p = 0.9$; genotype by paired-pulse interval: $F_{(9,513)} = 0.6$, $p = 0.8$; $n = 29$ for WT; $n = 30$ for DKO) (Fig. 3*D*).

In a short summary, our results demonstrate that Ca^{2+}-stimulated AC activity plays a critical role in both upregulation and downregulation of synaptic strength in the hippocampus.

Both initial and reversal spatial reference memory require Ca^{2+}-stimulated AC activity

Our previous study has found that AC1 is required for retention but not acquisition of spatial memory (Wu et al., 1995). Here, we used Morris water maze to examine both acquisition and memory retention in DKO mice. As shown in Figure 4*A*, we first trained animals to navigate in water and find the visible platform. Both WT and DKO mice showed significant improvement in escape latency during the 2 d training (Fig. 4*B*). Because both animal groups (i.e., WT and DKO mice) showed comparable performance in the cued/visible platform protocol preceding three different hidden platform training paradigms, the data shown in Figure 4*B* represented pooled results from all cued trainings. There is no significant difference between WT controls ($n = 33$) and DKO mutants ($n = 32$) (genotype: $F_{(1,63)} < 0.1$, $p > 0.8$; genotype by training trial: $F_{(7,441)} = 1.7$, $p = 0.1$; two-way repeated-measures ANOVA). Furthermore, WT and DKO animals showed similar swimming speed during the cued platform training (14.6 ± 0.6 cm/s for WT; 15.3 ± 0.4 cm/s for DKO mice; $p = 0.31$ between the two groups). These data indicate normal vision, locomotor skill, and motivation in DKO animals.

One day after the last trial of cued platform training, mice were trained to find the hidden platform by using the extra-maze spatial references (with protocol for WME-1). During the 12 d of initial hidden platform training (two trials per day with 4 h ITI), DKO mutants ($n = 16$) exhibited significantly longer escape latency to land on the initial hidden platform than WT controls ($n = 11$) (genotype: $F_{(1,25)} = 12.8$, $p = 0.001$; genotype by training day: $F_{(11,275)} = 2.3$, $p = 0.01$), although both groups showed significant improvement across the training sessions as indicated by the main effect of time (DKO, $F_{(11,165)} = 4.7$; WT, $F_{(11,110)} = 11.3$; $p < 0.001$ for both groups) (Fig. 4*C*). There was no significant group difference for swimming speed across the 12 d of training (WT, 12.4 ± 0.4 cm/s; DKO, 12.9 ± 0.5 cm/s; $p = 0.4$, unpaired *t* test). Furthermore, the degree of thigmotaxis as measured by percentage of time spending within a 8 cm zone around the wall was not significantly different between WT and DKO mice (genotype: $F_{(1,25)} = 2.3$, $p = 0.14$; genotype by training day: $F_{(11,275)} = 1.3$, $p = 0.24$) (data not shown). Therefore, the impaired acquisition in DKO mice was not due to defective locomotor ability or searching strategy.

As indicated in Figure 4*A*, we performed two probe trials to test memory retention: one after 6 d of training and another one after 12 d of training. For the time that both groups spent in quadrants during probe test trials (P1 and P2) (Fig. 4*D*), three-way repeated-measures ANOVA with probe trial and quadrant as within-subject factors revealed significant effects of quadrant ($F_{(3,75)} = 56.4$; $p < 0.001$) and the interaction of genotype with quadrant ($F_{(3,75)} = 4.7$; $p < 0.01$). Further analysis revealed both animal groups showed significant spatial preference to the target quadrant during both probe trials ($p < 0.05$ for P1, and $p < 0.01$ for P2, when comparing the target quadrant to other quadrants).

However, comparison between groups indicated that DKO mutants spent significantly less time in the target quadrant than WT controls during both probe trials ($p = 0.01$ for both trials, LSD test). There was no significant difference for the time spent in the nontarget quadrants between the two groups ($p > 0.05$). Furthermore, both animal groups showed significant improvement for the time spent in the target quadrant when comparing P2 to P1 ($p < 0.05$ for both WT and DKO). For the platform crossing number (Fig. 4*E*), the main effects of genotype ($F_{(1,25)} = 4.8$; $p < 0.05$) and probe trial ($F_{(1,25)} = 11.7$; $p < 0.01$) were significant. Although both groups showed improvement for the platform crossing number when comparing P2 with P1 (both $p < 0.05$), DKO mutants had fewer platform crossing times than WT mice in P2 ($p = 0.02$) rather than in P1 ($p = 0.4$). Crossing number of corresponding platform locations in other quadrants was similar between WT and DKO groups (all $p > 0.1$) (data not shown).

We next moved the platform to the opposite quadrant location (i.e., quadrant 3, as indicated in Fig. 4*G*) and performed reversal training. To find the new reversal platform location, animals need to establish new memory and in the meantime suppress the memory for the initial old platform location (i.e., quadrant 1, as indicated in Fig. 4*D*). During the 8 d of reversal platform training (two trials per day with an ITI of 4 h, as indicated in Fig. 4*A*), DKO mutants showed significantly longer escape latency to find the new reversal platform location than WT (genotype: $F_{(1,25)} = 8.0$, $p < 0.01$; genotype by training day: $F_{(7,175)} = 2.1$, $p = 0.05$) (Fig. 4*F*). For the quadrant time spent during the two probe trials of the reversal platform (i.e., P3 and P4) (Fig. 4*G*), three-way repeated-measures ANOVA revealed significant effects of quadrant ($F_{(3,75)} = 13.7$; $p < 0.001$) and the interaction between genotype and quadrant ($F_{(3,75)} = 14.7$; $p < 0.001$). WT controls showed preference to the new target quadrant during both probe trials (all $p < 0.01$, pairwise LSD comparisons between the new quadrant and the other quadrants), indicating that WT animals efficiently suppressed the old spatial memory and established new memory for the reversal platform location. Strikingly, although DKO mutants showed weaker initial memory for the old platform (Fig. 4*D*,*E*), reversal training did not efficiently suppress their old spatial memory. In probe test 3 (Fig. 4*G*), DKO mutants still exhibited preference to the old target quadrant (i.e., quadrant 1) ($p < 0.05$ when comparing quadrant 1 to the other quadrants), and they did not show preference to the new target quadrant ($p > 0.2$ when comparing quadrant 3 to the two adjacent quadrants). After additional 4 d of reversal training, DKO mice showed a tendency of spending more time in the new quadrant ($p < 0.01$ between quadrant 3 and 2; $p = 0.06$ between quadrant 3 and 4; $p > 0.1$ between quadrant 3 and 1). Although DKO did not show preference to the old platform in

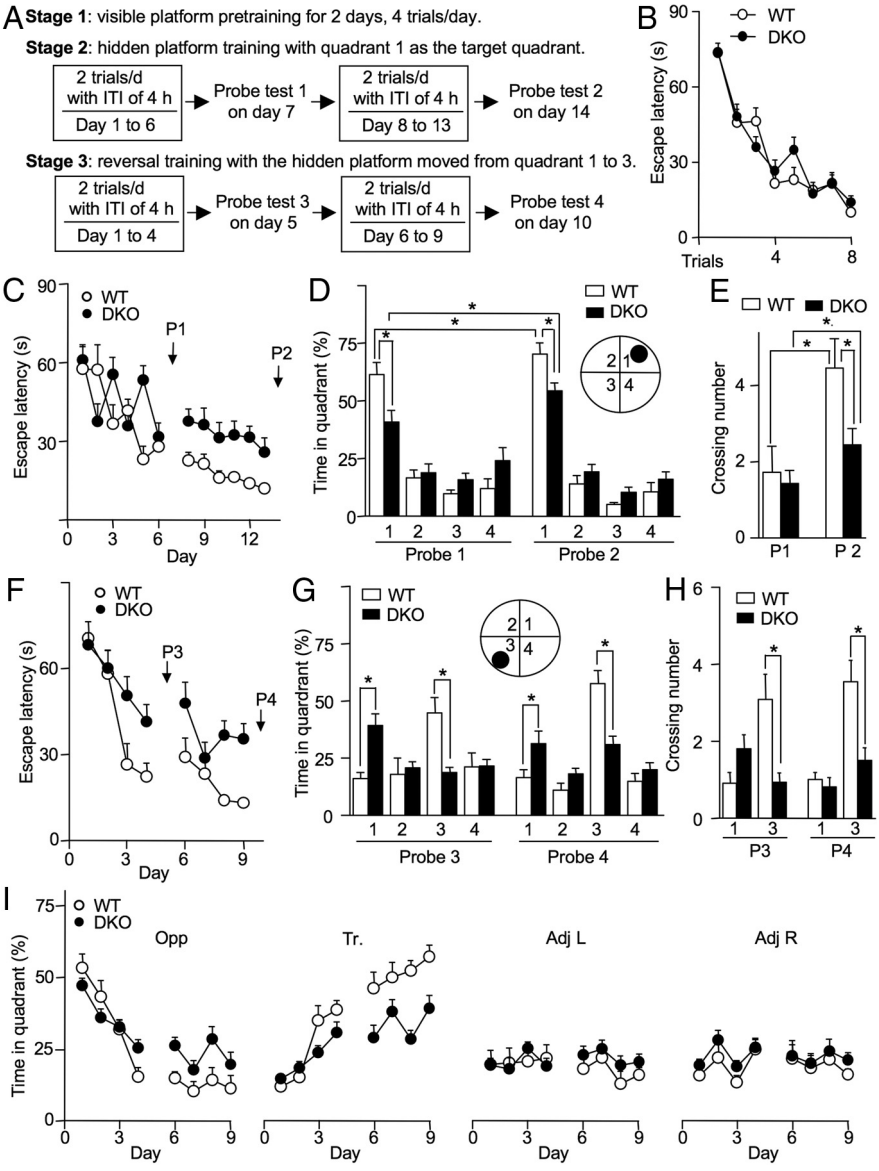

Figure 4. Acquisition and retention of spatial information require Ca^{2+}-stimulated AC. ***A***, Experimental layout of Morris water maze experiment 1 (MWE-1). Mice were first trained to find the cued/visible platform (stage 1). Then, they were trained to find the hidden platform (stage 2). Two probe tests (P1 and P2) were performed halfway and at the end of the hidden platform training sessions, respectively. In the third stage, mice were trained by reversal trials. Two probe tests (P3 and P4) were performed as indicated. ***B***, WT ($n = 33$) and DKO ($n = 32$) mice showed comparable performance during the cued platform training. ***C***, DKO mutants ($n = 16$) showed spatial learning defects to find the initial hidden platform when compared with WT mice ($n = 11$). Data of two training trials on each day were combined for analysis. P1 and P2 represent the first and second probe test, respectively. ***D***, DKO mutants showed less preference to the target quadrant (i.e., quadrant 1 as indicated) than WT mice in both probe tests. ***E***, DKO mutants showed less crossing over the initial platform location than WT mice in the second but not in the first probe test. ***F***, DKO mutants showed defective reversal learning to find the new platform location when compared with WT mice. ***G***, DKO mutants spent significantly less time in new target quadrant (i.e., quadrant 3) ($p < 0.05$ for both probe tests), but more time in the old target quadrant (i.e., quadrant 1) when compared with WT mice ($p < 0.05$ for both probe tests). ***H***, DKO mutants showed fewer crossing over the new target location ($p < 0.05$ for both probe tests). ***I***, Data for the percentage of time spent in each quadrant during each day of the reversal training. Opp., The old and initial target quadrant; Tr., the new target quadrant for the reversal training; Adj L, left quadrant adjacent to the old target; Adj R, right quadrant adjacent to the old quadrant. *$p < 0.05$ between the indicated groups. Error bars indicate SEM.

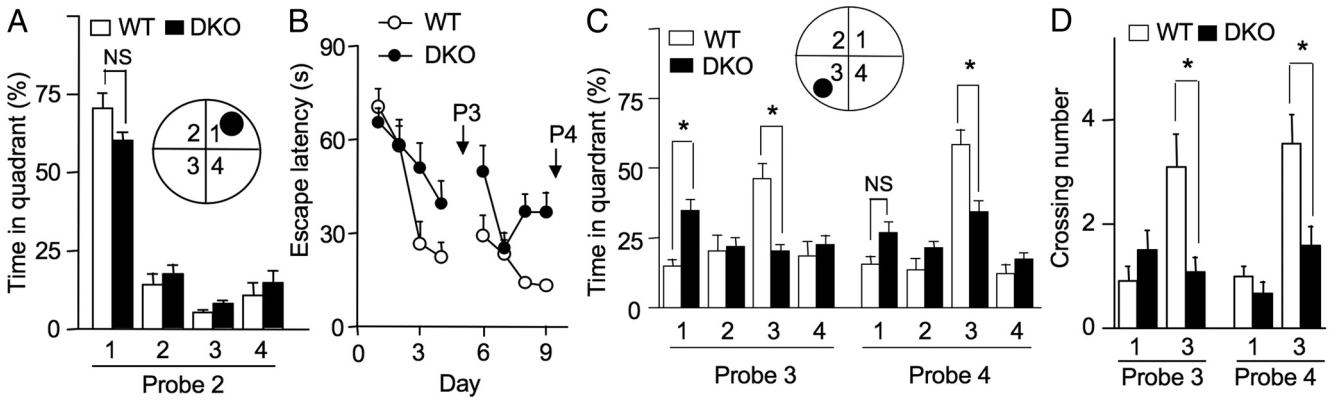

Figure 5. Subpopulation of DKO mice, which show normal initial memory, displays defective reversal learning. Although majority of DKO mice (12 of 16 mice trained by MWE-1 in Fig. 4) showed significant improvement during probe test 2 after 6 d of additional training (from day 8 to 13), 4 DKO mice did not show any crossing over the initial platform location in probe 2. After excluding these 4 DKO animals, the percentage of time spent in each quadrant was comparable between DKO ($n = 12$) and WT mice (***A***). When data from these animals were reanalyzed for escape latency during the reversal training (***B***), probe tests for the reversal platform (***C***), and crossing number over the reversal platform location (i.e., the platform in quadrant 3) (***D***), these DKO mice displayed similar deficits as those shown in Figure 4. NS, Not statistically significant between the indicated groups. *$p < 0.05$ between the indicated groups. Error bars indicate SEM.

probe test 4 (both $p > 0.1$ when compared between quadrant 1 and the two adjacent quadrants), they spent significantly more time in the old target quadrant but less time in the new target quadrant than the WT controls during both probe test 3 and 4 ($p < 0.05$) (Fig. 4*G*). For new and old platform crossing number, there were significant main effects of genotype ($F_{(1,25)} = 19.8$) and quadrant ($F_{(1,25)} = 17.6$), and of the interaction between genotype and quadrant ($F_{(1,25)} = 20.7$; $p < 0.01$ for all cases). DKO mutants showed fewer crossing number over new platform location during both probe trials than WT controls (both $p < 0.01$) (Fig. 4*H*). The crossing numbers over the old platform location were comparable between the two groups ($p = 0.08$ for P3; $p = 0.6$ for P4).

The finding that DKO mutants spent more time in the old target quadrant but less time in the new target quadrant during probe trials suggested that such phenotype might also happen during the reversal platform training sessions. Therefore, we did further data analysis on the time that both groups spent in each quadrant during the reversal training sessions. As shown in Figure 4*I*, both animal groups gradually decreased their time searching in the old target quadrant and increased searching time in the new target quadrant (within-subject effects of time, $p < 0.001$ for both groups). The searching time spent in the nontarget quadrants (i.e., adjacent left and right quadrants) remained almost stable for both WT and DKO mice (Fig. 4*I*). However, DKO mutants showed slower percentage time decrease searching in the old target quadrant (genotype by training day: $F_{(7,175)} = 2.9$, $p < 0.01$), as well as slower percentage time increase searching the new target quadrant (genotype by training day: $F_{(7,175)} = 4.2$, $p < 0.01$). These data suggested that the balance of new memory formation and old memory suppression might be shifted to favor the perseverance of old memory in DKO animals under this particular training paradigm (two trials each day with ITI of 4 h).

One complication for the impaired reversal learning in DKO mice is that their memory for the initial platform (i.e., old platform) is weaker than the WT animals. It is conceivable that weaker initial memory should be easier to suppress. The impaired reversal of the weaker initial memory in DKO mice may already indicate a severe dysfunction of relearning/old memory suppression. However, a fair examination should be done with animals that show equivalent strength of initial memory. Therefore, we reanalyzed the data by excluding the poor performers from the DKO group. We noticed that four DKO mice did not show any platform crossing over the initial platform during probe test 2. After excluding these four DKO mice, this subpopulation of DKO mice displayed comparable performance in probe test 2 to that of the WT group (Fig. 5*A*) (70.4 ± 4.8% for WT and 60 ± 2.7% for DKO; $p > 0.1$). When data from these animals were reanalyzed for the performance during the reversal learning and the subsequent probe tests (i.e., P3 and P4), it appeared that DKO mice showed similar performance profile to that presented in Figure 4. They were impaired for relearning (Fig. 5*B*) ($F_{(1,21)} = 7.8$; $p < 0.05$), new memory establishment (Fig. 5*C*,*D*) (DKO mice showed significant less preference to the new platform location than WT mice, $F_{(3,63)} = 17.6$, $p < 0.01$), and the suppression of the old spatial memory (DKO but not WT mice spent significantly more time in the old target quadrant during probe test 3; $p < 0.05$) (Fig. 5*C*). These data further support that Ca^{2+}-stimulated AC is important for memory reversal, which requires both new learning and suppression of old memories. However, because of the intrinsic features of this particular training paradigm, it is difficult to dissect whether the preference to the old target in DKO mice is due to direct effects of memory suppression or due to less competition from new memory establishment.

Extinction of the old spatial memory is impaired in DKO mutants

To minimize the competition effects from learning the new platform location, we chose to examine the suppression of the old spatial memories by using an extinction paradigm (Lattal et al., 2003; Suzuki et al., 2004). Following the protocol described as WME-2 in Materials and Methods, we first trained new cohorts of mice by a more intensive training (four trials per day with ITI of 30 min, as illustrated in Fig. 6*A*) with the attempt to achieve strong and comparable memory in both WT and DKO groups. DKO mice showed slower improvement of escape latency during the whole training process ($F_{(1,16)} = 14.6$; $p < 0.01$) (Fig. 6*B*). Although DKO mice showed weaker memory after 24 trials of hidden platform training (from day 1 to day 6), they displayed comparable memory retention to that of WT group after additional 3 d of training. Specifically, when tested by a probe trial on day 7, DKO mutants spent significantly less time in the target quadrant (DKO, 32.7 ± 7.1%; WT, 50.3 ± 3.8%; $p = 0.03$) (Fig. 6*C*). The number of crossing over the platform location was also

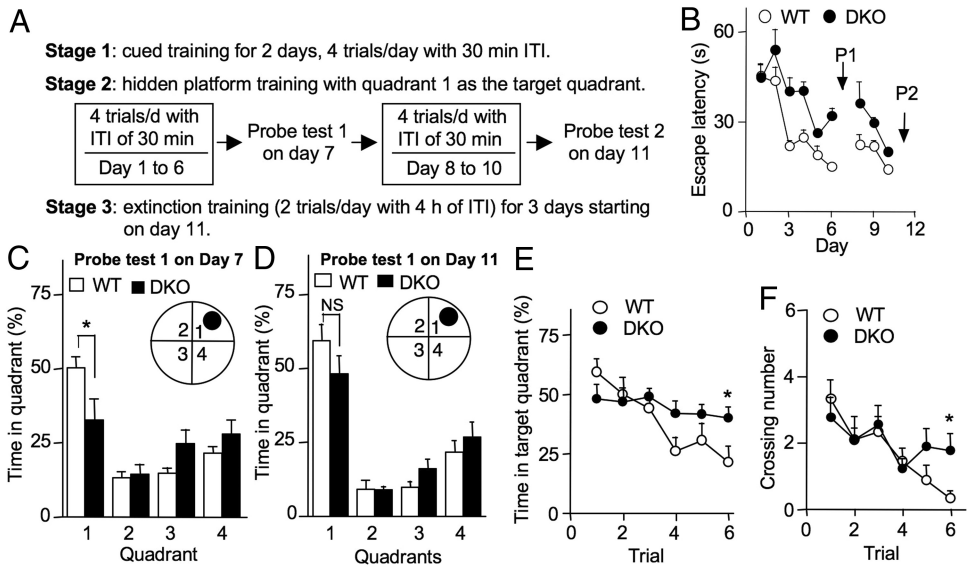

Figure 6. Spatial memory extinction requires Ca^{2+}-stimulated AC. ***A***, Illustration of the training protocols for the water maze experiment 2 (WME-2). Animals were first pretrained by cued/visible platform trials, followed by hidden platform training. Probe tests were used to examine the strength of memory retention. After both WT and DKO mice showed significant memory formation, they were subjected to extinction trials, during which animals were allowed to swim in the pool without any platform for 60 s. ***B***, DKO mutants ($n = 9$) showed longer escape latencies during the hidden platform training than their WT controls ($n = 9$). ***C***, During probe test 1 performed after 6 d of hidden platform training, only WT but not DKO mice showed robust memory formation for the platform location (quadrant 1 as indicated). ***D***, DKO mutants showed comparable memory formation to that of WT mice during probe test 2 after training for 3 additional days. ***E***, After 3 d of extinction training (2 trials per day), WT mice no longer showed preference for the target quadrant. In contrast, DKO mice showed preference, indicating deficits in memory extinction. ***F***, WT but not DKO mice showed significant decrease in crossing over the platform location during the six extinction trials. $*p < 0.05$ between DKO and WT groups. NS, Not statistically significant between the indicated groups. Error bars indicate SEM.

fewer than WT controls (DKO, 1.4 ± 0.5; WT, 3.8 ± 0.7; $p = 0.02$, unpaired t test). After an additional 12 training trials (four trials per day for 3 d), DKO and WT animals showed comparable preference to the target quadrant in the second probe test (P2 on day 11) (DKO, 48% ± 6.2; WT, 59% ± 5.5%; $p = 0.19$) (Fig. 6*D*).

Following the second probe test, which was considered as the fist extinction session, animals were reintroduced to the pool without the presence of the platform 4 h later. This particular extinction paradigm was repeated for 2 additional days. During these six probe/extinction trials, animals would suppress the previously established memory and show decrease in time spent in the target quadrant. As shown in Figure 6*E*, WT ($F_{(5,40)} = 7.7$; $p < 0.001$) but not DKO mice ($F_{(5,40)} = 0.8$; $p = 0.59$) displayed significant decrease in the time spent in the trained quadrant across all extinction sessions. There was also a significant interaction effect between genotype and training trial ($F_{(5,80)} = 2.8$; $p = 0.02$). Consistently, WT ($F_{(5,40)} = 10.0$; $p < 0.001$) but not DKO mice ($F_{(5,40)} = 1.1$; $p = 0.38$) significantly reduced their crossing number over the trained platform location (Fig. 6*F*). After six extinction trials, the preference to the target quadrant reduced to chance level (21.4 ± 6.9%) in WT mice. However, DKO mice showed stronger preference (40.2 ± 4.7%) to the target quadrant than WT animals ($p < 0.05$). DKO mice also showed more crossing number over the trained platform location in the sixth extinction session than WT (DKO, 1.78 ± 0.52; WT, 0.33 ± 0.23; $p < 0.05$). These data suggest that efficient suppression of the obsolete spatial memory requires Ca^{2+}-stimulated AC activity.

Pretraining with visible platform does not affect subsequent formation of reference spatial memory

It has been shown that previous spatial training may affect subsequent learning, during which animals are exposed to new spatial cues (Bannerman et al., 1995). Although, in our experimental setup, mice during the visible platform pretraining should not be significantly influenced by the extra-maze reference cues, we further tested whether Ca^{2+}-stimulated AC regulates spatial memory formation without any form of pretraining. A new cohort of naive WT and DKO mice was directly subjected to hidden platform training (described as WME-3 in Material and Methods). Except for no visible platform training, these animals experienced same hidden platform training as those in WME-2 (Fig. 6*B–D*). As shown in Figure 7*A*, DKO mice displayed slower improvement of escape latency than WT mice ($p < 0.05$). Compared with WT mice, DKO mutants did not show preference to the hidden platform location in probe test 1 (on day 7 after 6 d of training) (Fig. 7*B*,*C*) ($p < 0.05$). After additional 3 d of training, DKO mice showed comparable memory to that of WT mice in probe test 2 (Fig. 7*B*,*C*). When these results were compared with data collected from animals in WME-2, which were pretrained with visible platform (in Fig. 6*C*,*D*), it appeared that the performance of WT, as well as DKO mice, was similar in the probe tests regardless of previous experience with visible platform ($p > 0.05$ between pertained and non-pretrained WT; $p > 0.05$ between pretrained and non-pretrained DKO).

Spatial learning and memory deficits in DKO mutants can be partially rescued by trainings with compressed intertrial interval

Because HFS with compressed intertetanus interval (i.e., 1 min) rather than spaced interval (i.e., 5 min) successfully induced LTP in DKO (Fig. 2*B*), it is possible that DKO mice form normal spatial memory after trainings with compressed ITI. By using a protocol described as WME-4 in Materials and Methods, new cohorts of WT and DKO mice were first trained to find the visible platform, and then trained by four trials per day with 1 min ITI to find the hidden platform. As shown in Figure 8*A*, DKO mice

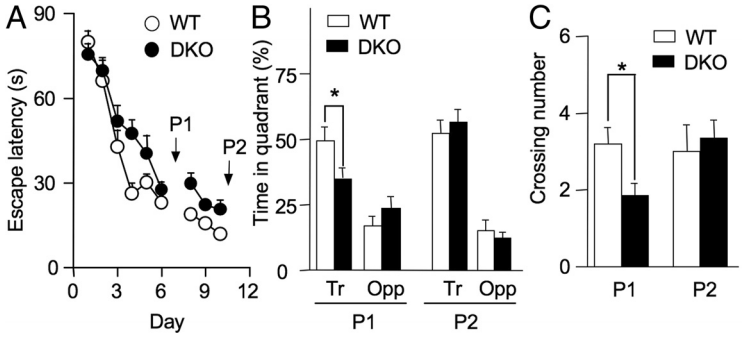

Figure 7. Without visible platform pretraining, DKO mice still show defective spatial memory formation. Naive WT ($n = 9$) and DKO mice ($n = 14$) were trained to use the extra-maze spatial cues to find the hidden platform location without visible platform pretraining. Mice were trained by four trials per day with ITI of 30 min for 6 d. Then, a probe test (P1) was performed on day 7. Next, these mice were further trained for another 3 d (from day 8 to 10), and a second probe test (P2) was performed on day 11. Compared with WT mice, DKO mutants showed slower improvement of escape latency during the hidden platform trainings (***A***), less preference to the target quadrant in probe test 1 but not probe test 2 (***B***), and less crossing over the hidden platform location in probe test 1 but not probe test 2 (***C***). Tr, Target quadrant; Opp, opposite quadrant. *$p < 0.05$ between DKO and WT groups. Error bars indicate SEM.

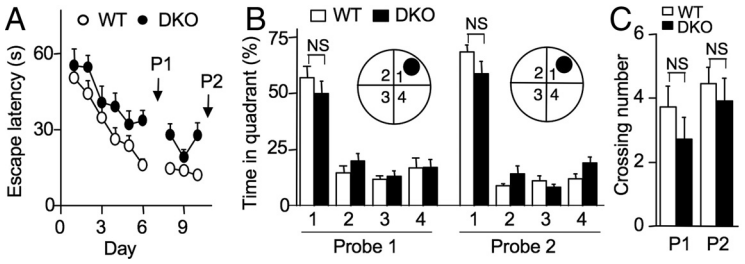

Figure 8. Hidden platform trainings with compressed ITI improve spatial memory in DKO mice. WT ($n = 10$) and DKO ($n = 10$) animals were first pretrained with the visible platform paradigm as described in Materials and Methods. Then, they were trained by four trials per day with ITI of 1 min to find the hidden platform for 6 d. They were examined by the first probe test (P1) on day 7, further trained for 3 more days (from day 8 to 10), and examined by another probe test (P2) on day 11. Although DKO mice showed slower improvement in escape latency during the hidden platform training (***A***), they showed comparable preference to the target quadrant (i.e., quadrant 1 as indicated) in both probe tests (***B***), and similar number of crossing over the platform location to that of WT group (***C***). NS, Not statistically significant between the indicated groups. Error bars indicate SEM.

showed slower improvement of escape latency during the whole training process than WT animals (genotype: $F_{(1,18)} = 8.2$, $p = 0.01$). However, DKO mice showed comparable performance to that of WT mice in both probe tests (as indicated by P1 and P2 in Fig. 8). Both WT and DKO mice showed significant preference to the target quadrant ($F_{(3,54)} = 75.7$; $p < 0.001$), and there were no significant genotype effects (all $p > 0.1$) on quadrant time (Fig. 8*B*) or on platform crossing numbers (Fig. 8*C*). We further compared the probe test performance of DKO mutants with data collected from water maze experiment 2 (described as WME-2 in Materials and Methods) (results shown in Fig. 6*C*,*D*). The hidden platform training strategies of WME-4 and WME-2 are essentially the same except that the ITI is 1 min for WME-4 and 30 min for WME-2. After 6 d of hidden platform training, DKO mutants trained with compressed ITI in WME-4 spent significantly more time in the target quadrant (48.5 ± 5.9%) than the DKO group trained with spaced ITI in WME-2 (30.0 ± 5.4%; $p < 0.05$, unpaired *t* test) in probe test 1. Additionally, DKO mice formed WT-level memory during probe test 2 after another 3 d of training (from day 8 to 10) regardless of using compressed or spaced ITI (Figs. 6*D*, 8*B*). These data show that the deficits in DKO mice can be partially rescued by either training with compressed ITI or overtraining (i.e., additional 3 d of training in WME-2).

Discussion

The requirement of cAMP–PKA signaling for the maintenance of late-phase LTP has been extensively elucidated (Frey et al., 1993; Nguyen et al., 1994; Abel et al., 1997). Our previous study with hippocampal slices has demonstrated that lack of AC1/AC8 in mice causes defective LTP maintenance without affecting induction (Wong et al., 1999). Because previous reports have suggested that the requirement of cAMP–PKA signaling in early-phase LTP (E-LTP) may depend on the induction protocol (Blitzer et al., 1995; Otmakhova et al., 2000; Woo et al., 2003), we decided to further investigate the function of Ca^{2+}-stimulated AC in LTP induction (i.e., E-LTP). Nguyen and Kandel (1997) reported that E-LTP induced by multiple theta-burst stimulations does not require PKA. In contrast, a PKA inhibitor H89 (*N*-[2-[[3-(4-bromophenyl)-2-propenyl]amino]ethyl]-5-isoquinolinesulfonamide dihydrate dihydrochloride) significantly suppresses E-LTP induced by a single train of tetanus (100 Hz for 1 s) (Otmakhova et al., 2000). Supportively, DKO mice displayed normal E-LTP induced by multiple trains of HFS (four 200 ms tetanic trains at 100 Hz with ITI of 6 s), as demonstrated by our previous report (Wong et al., 1999). Interestingly, a single train of HFS (100 Hz, 1 s) failed to induce LTP in DKO mice (this study). These data extend our understanding on the function of Ca^{2+}-stimulated cAMP signaling in both induction and maintenance of LTP.

Another finding of this study is that the induction of E-LTP in DKO mice by two trains of high-frequency stimulation (at 100 Hz) depends on the intertetanus interval. Previous studies have suggested a temporal sensitivity of cAMP for LTP induction. While LTP induced by multiple stimulations with spaced intervals (such as 300 or 80 s) can be blocked by pharmacological or genetic reduction of PKA activity, the induction of LTP by multiple stimulations with massed (or compressed) intervals (such as 3, 20, or 40 s) does not require PKA (Woo et al., 2003; Kim et al., 2010). A simulation model provided by Kim et al. (2010) predicts that the critical intertetanus interval for PKA-dependent LTP is ~60 s, and the requirement of PKA under spaced tetanic condition is to compensate for a decrease of CaMKII activation after spaced stimulation. This mechanism may also explain why E-LTP induced by HFS at 200 Hz is normal in DKO mice. If 200 Hz HFS stimulates more persistent CaMKII activation than 100 Hz, cAMP and PKA may be less critical for LTP induction. These studies, as well as our data, suggest interesting cross talks of different Ca^{2+}-stimulated signaling pathways with the function of time-dependent relay in the establishment of synaptic potentiation. Other Ca^{2+}-stimulated signaling pathways, such as calmodulin-dependent kinases (CaMKs) (Wayman et al., 2008) and extracellular signal-regulated kinases (ERKs) (Schmitt et al., 2005), may also be recruited during LTP induction. When stronger stimulation is used

to induce LTP (such as HFS at 200 Hz or multiple titanic stimulations with compressed interval), higher activation of other Ca^{2+}-stimulated kinases (such as ERK and CaMKs) may compensate for the loss of Ca^{2+}-stimulated cAMP elevation. Interestingly, the stimulation intensity- and interval-dependent effects were also observed when examining spatial memory formation. Specifically, we found that DKO mice showed normal memory formation after more extensive training (i.e., four trials per day for 9 d vs four trials per day for 6 d) or trainings with compressed ITI (i.e., four trials per day with 1 min ITI for 6 d vs four trials per day with 30 min ITI for 6 d).

The present work demonstrates that LTD in live adult mice requires Ca^{2+}-stimulated AC. This finding extends a previous study that *in vitro* slices from juvenile AC8 KO mice fail to develop LTD (Schaefer et al., 2000). The requirement of Ca^{2+}-stimulated cAMP production for LTD is consistent with the function of PKA in *de novo* synaptic depression (Brandon et al., 1995; Qi et al., 1996). While the establishment of LTP reflects activity-dependent synaptic strengthening, the reversal of the potentiated synapses (i.e., depotentiation) represents an attractive cellular model to study how previously strengthened synapses can be destrengthened. Although LTD and depotentiation may involve different molecular mechanisms (Lee et al., 2000; Li et al., 2007), our data and other studies demonstrate the function of Ca^{2+}-stimulated cAMP–PKA signaling in both processes. For example, genetic disruption of R1β or Cβ1 subunit of PKA causes impaired LTD and depotentiation in hippocampal slices (Brandon et al., 1995; Qi et al., 1996). However, a recent report supports that the reduction of PKA activity facilitates LTD consolidation (Malleret et al., 2010). Alternatively, Ca^{2+}-stimulated AC may impinge on the Epac–Rap–p38–MAPK signaling and regulate LTD in a PKA-independent manner (Ster et al., 2009). Therefore, it is possible that the loss of Ca^{2+}-stimulated AC activity may lead to more severe disruption of the intracellular signaling by affecting multiple downstream targets. One question is how Ca^{2+}-stimulated AC can bidirectionally regulate synaptic plasticity (i.e., both potentiation and depression/depotentiation). One possibility is that cAMP signaling may affect different downstream targets, which are distinctly activated by HFS and LFS. Such scenario is implicated in ERK signaling. While ERK activity stimulates CREB during LTP (Adams and Sweatt, 2002), it activates Elk but not CREB during LTD (Thiels et al., 2002).

Although the function of both PKA and AC1 has been demonstrated in spatial memory formation (Wu et al., 1995; Abel et al., 1997), how Ca^{2+}-stimulated cAMP signaling regulates relearning and suppression of old spatial memory is largely unknown. An immunohistochemistry study has documented dynamic changes of PKA activity during training and reversal training with Y-maze (Havekes et al., 2007). After the first reversal training session, PKA RIIα, β level is increased in the DG and CA3 regions. After the third training session, during which animals have not fully established the new reversal memory, an increase in RIIα, β is observed in the CA1 region. The immunoreactivity returns to the baseline level at the end of the training (after the seventh training). Although the functional relevance for the transient changes of PKA level is unclear, we observed dramatic deficits in DKO mice during the reversal training sessions. After the first 4 d of training, only WT mice showed preference for the new target quadrant. DKO mice still showed preference for the old rather than the new platform location. Although the data in Figure 4 suggested that the effective suppression of old spatial memory might depend on Ca^{2+}-stimulated AC, it is possible that the phenotype is due to less competition from new spatial learning. However, we found that the old spatial memory in DKO was more resistant to extinction trainings. Therefore, we conclude that both relearning and old spatial memory suppression require Ca^{2+}-stimulated cAMP signaling.

It appears that suppression of old spatial memory and old fear memory (or fear extinction) may be mechanistically different. Although Szapiro et al. (2003) demonstrated that infusion of PKA inhibitor Rp-cAMPs [(*R*)-adenosine, cyclic 3′,5′-(hydrogen phosphorothioate)triethylammonium] into the hippocampus impaired extinction of fear in the step-down avoidance paradigm, genetic suppression of PKA activity in the forebrain facilitated extinction of contextual fear (Isiegas et al., 2006). Isiegas et al. (2006) used genetic approaches to overexpress R(AB) in young adult mice, in which PKA activity reduced by ~20%. These R(AB) transgenic animals showed normal retrieval but faster extinction of contextual memory. Consistent with this finding, we previously reported that AC1-overexpressing mice, which had ~30% more PKA activity in the hippocampus, showed slower extinction of contextual fear memory (Wang et al., 2004). In another study, Monti et al. (2006) delivered a phosphodiesterase inhibitor rolipram to increase cAMP into the brain. They found that, after training by tone–footshock paring and during the multiple extinction sessions, rolipram-infused rats displayed more retention and slower extinction.

In summary, this study implicates a novel requirement of Ca^{2+}-stimulated AC for the flexibility of both synaptic modification and memory formation/suppression. Although our data showed a correlation between defective synaptic depression/depotentiation and impaired old memory suppression in DKO mice, it is a challenge to demonstrate direct causal effects of these synaptic abnormalities on behavior. While an early study has reported an association between defective reversal spatial learning and impaired LTD rather than depotentiation (Nicholls et al., 2008), other evidence has suggested that synaptic depotentiation in amygdala may account for fear memory extinction (Kim et al., 2007). Additionally, old memory suppression or extinction may rely on brain areas distinct from the hippocampus (such as prefrontal cortex). Although our study did not focus on prefrontal cortex, previous reports have shown that upregulation of cAMP–PKA signaling is associated with LTP in prefrontal cortex (Jay et al., 1998; Hotte et al., 2007). It remains to determine whether memory extinction involves coordination between LTP in prefrontal cortex and LTD/depotentiation in hippocampus, or coordination between LTP in unexperienced neurons and LTD/depotentiation in previously potentiated neurons.

References

Abel T, Nguyen PV (2008) Regulation of hippocampus-dependent memory by cyclic AMP-dependent protein kinase. Prog Brain Res 169:97–115.

Abel T, Nguyen PV, Barad M, Deuel TA, Kandel ER, Bourtchouladze R (1997) Genetic demonstration of a role for PKA in the late phase of LTP and in hippocampus-based long-term memory. Cell 88:615–626.

Adams JP, Sweatt JD (2002) Molecular psychology: roles for the ERK MAP kinase cascade in memory. Annu Rev Pharmacol Toxicol 42:135–163.

Bannerman DM, Good MA, Butcher SP, Ramsay M, Morris RG (1995) Distinct components of spatial learning revealed by prior training and NMDA receptor blockade. Nature 378:182–186.

Blitzer RD, Wong T, Nouranifar R, Iyengar R, Landau EM (1995) Postsynaptic cAMP pathway gates early LTP in hippocampal CA1 region. Neuron 15:1403–1414.

Bouton ME (2004) Context and behavioral processes in extinction. Learn Mem 11:485–494.

Brandon EP, Zhuo M, Huang YY, Qi M, Gerhold KA, Burton KA, Kandel ER, McKnight GS, Idzerda RL (1995) Hippocampal long-term depression

and depotentiation are defective in mice carrying a targeted disruption of the gene encoding the RI beta subunit of cAMP-dependent protein kinase. Proc Natl Acad Sci U S A 92:8851–8855.

Braunewell KH, Manahan-Vaughan D (2001) Long-term depression: a cellular basis for learning? Rev Neurosci 12:121–140.

Diamond DM, Park CR, Campbell AM, Woodson JC (2005) Competitive interactions between endogenous LTD and LTP in the hippocampus underlie the storage of emotional memories and stress-induced amnesia. Hippocampus 15:1006–1025.

Eckel-Mahan KL, Phan T, Han S, Wang H, Chan GC, Scheiner ZS, Storm DR (2008) Circadian oscillation of hippocampal MAPK activity and cAMP: implications for memory persistence. Nat Neurosci 11:1074–1082.

Frey U, Huang YY, Kandel ER (1993) Effects of cAMP simulate a late stage of LTP in hippocampal CA1 neurons. Science 260:1661–1664.

Havekes R, Timmer M, Van der Zee EA (2007) Regional differences in hippocampal PKA immunoreactivity after training and reversal training in a spatial Y-maze task. Hippocampus 17:338–348.

Heynen AJ, Abraham WC, Bear MF (1996) Bidirectional modification of CA1 synapses in the adult hippocampus in vivo. Nature 381:163–166.

Heynen AJ, Quinlan EM, Bae DC, Bear MF (2000) Bidirectional, activity-dependent regulation of glutamate receptors in the adult hippocampus in vivo. Neuron 28:527–536.

Hotte M, Thuault S, Dineley KT, Hemmings HC Jr, Nairn AC, Jay TM (2007) Phosphorylation of CREB and DARPP-32 during late LTP at hippocampal to prefrontal cortex synapses in vivo. Synapse 61:24–28.

Huang CC, Hsu KS (2001) Progress in understanding the factors regulating reversibility of long-term potentiation. Rev Neurosci 12:51–68.

Isiegas C, Park A, Kandel ER, Abel T, Lattal KM (2006) Transgenic inhibition of neuronal protein kinase A activity facilitates fear extinction. J Neurosci 26:12700–12707.

Jay TM, Gurden H, Yamaguchi T (1998) Rapid increase in PKA activity during long-term potentiation in the hippocampal afferent fibre system to the prefrontal cortex in vivo. Eur J Neurosci 10:3302–3306.

Kim J, Lee S, Park K, Hong I, Song B, Son G, Park H, Kim WR, Park E, Choe HK, Kim H, Lee C, Sun W, Kim K, Shin KS, Choi S (2007) Amygdala depotentiation and fear extinction. Proc Natl Acad Sci U S A 104:20955–20960.

Kim M, Huang T, Abel T, Blackwell KT (2010) Temporal sensitivity of protein kinase a activation in late-phase long term potentiation. PLoS Comput Biol 6:e1000691.

Lattal KM, Mullen MT, Abel T (2003) Extinction, renewal, and spontaneous recovery of a spatial preference in the water maze. Behav Neurosci 117:1017–1028.

Lee HK, Barbarosie M, Kameyama K, Bear MF, Huganir RL (2000) Regulation of distinct AMPA receptor phosphorylation sites during bidirectional synaptic plasticity. Nature 405:955–959.

Lee YS, Bailey CH, Kandel ER, Kaang BK (2008) Transcriptional regulation of long-term memory in the marine snail *Aplysia*. Mol Brain 1:3.

Li R, Huang FS, Abbas AK, Wigström H (2007) Role of NMDA receptor subtypes in different forms of NMDA-dependent synaptic plasticity. BMC Neurosci 8:55.

Malleret G, Alarcon JM, Martel G, Takizawa S, Vronskaya S, Yin D, Chen IZ, Kandel ER, Shumyatsky GP (2010) Bidirectional regulation of hippocampal long-term synaptic plasticity and its influence on opposing forms of memory. J Neurosci 30:3813–3825.

Monti B, Berteotti C, Contestabile A (2006) Subchronic rolipram delivery activates hippocampal CREB and arc, enhances retention and slows down extinction of conditioned fear. Neuropsychopharmacology 31:278–286.

Myers KM, Ressler KJ, Davis M (2006) Different mechanisms of fear extinction dependent on length of time since fear acquisition. Learn Mem 13:216–223.

Nguyen PV, Kandel ER (1997) Brief theta-burst stimulation induces a transcription-dependent late phase of LTP requiring cAMP in area CA1 of the mouse hippocampus. Learn Mem 4:230–243.

Nguyen PV, Woo NH (2003) Regulation of hippocampal synaptic plasticity by cyclic AMP-dependent protein kinases. Prog Neurobiol 71:401–437.

Nguyen PV, Abel T, Kandel ER (1994) Requirement of a critical period of transcription for induction of a late phase of LTP. Science 265:1104–1107.

Nicholls RE, Alarcon JM, Malleret G, Carroll RC, Grody M, Vronskaya S, Kandel ER (2008) Transgenic mice lacking NMDAR-dependent LTD exhibit deficits in behavioral flexibility. Neuron 58:104–117.

Otmakhova NA, Otmakhov N, Mortenson LH, Lisman JE (2000) Inhibition of the cAMP pathway decreases early long-term potentiation at CA1 hippocampal synapses. J Neurosci 20:4446–4451.

Qi M, Zhuo M, Skalhegg BS, Brandon EP, Kandel ER, McKnight GS, Idzerda RL (1996) Impaired hippocampal plasticity in mice lacking the Cβ1 catalytic subunit of cAMP-dependent protein kinase. Proc Natl Acad Sci U S A 93:1571–1576.

Schaefer ML, Wong ST, Wozniak DF, Muglia LM, Liauw JA, Zhuo M, Nardi A, Hartman RE, Vogt SK, Luedke CE, Storm DR, Muglia LJ (2000) Altered stress-induced anxiety in adenylyl cyclase type VIII-deficient mice. J Neurosci 20:4809–4820.

Schmitt JM, Guire ES, Saneyoshi T, Soderling TR (2005) Calmodulin-dependent kinase kinase/calmodulin kinase I activity gates extracellular-regulated kinase-dependent long-term potentiation. J Neurosci 25:1281–1290.

Shan Q, Chan GC, Storm DR (2008) Type 1 adenylyl cyclase is essential for maintenance of remote contextual fear memory. J Neurosci 28:12864–12867.

Silva AJ (2003) Molecular and cellular cognitive studies of the role of synaptic plasticity in memory. J Neurobiol 54:224–237.

Sindreu CB, Scheiner ZS, Storm DR (2007) Ca^{2+}-stimulated adenylyl cyclases regulate ERK-dependent activation of MSK1 during fear conditioning. Neuron 53:79–89.

Ster J, de Bock F, Bertaso F, Abitbol K, Daniel H, Bockaert J, Fagni L (2009) Epac mediates PACAP-dependent long-term depression in the hippocampus. J Physiol 587:101–113.

Suzuki A, Josselyn SA, Frankland PW, Masushige S, Silva AJ, Kida S (2004) Memory reconsolidation and extinction have distinct temporal and biochemical signatures. J Neurosci 24:4787–4795.

Szapiro G, Vianna MR, McGaugh JL, Medina JH, Izquierdo I (2003) The role of NMDA glutamate receptors, PKA, MAPK, and CAMKII in the hippocampus in extinction of conditioned fear. Hippocampus 13:53–58.

Thiels E, Kanterewicz BI, Norman ED, Trzaskos JM, Klann E (2002) Long-term depression in the adult hippocampus in vivo involves activation of extracellular signal-regulated kinase and phosphorylation of Elk-1. J Neurosci 22:2054–2062.

Wang H, Storm DR (2003) Calmodulin-regulated adenylyl cyclases: cross talk and plasticity in the central nervous system. Mol Pharmacol 63:463–468.

Wang H, Ferguson GD, Pineda VV, Cundiff PE, Storm DR (2004) Overexpression of type-1 adenylyl cyclase in mouse forebrain enhances recognition memory and LTP. Nat Neurosci 7:635–642.

Wayman GA, Lee YS, Tokumitsu H, Silva AJ, Soderling TR (2008) Calmodulin-kinases: modulators of neuronal development and plasticity. Neuron 59:914–931.

Wieczorek L, Maas JW Jr, Muglia LM, Vogt SK, Muglia LJ (2010) Temporal and regional regulation of gene expression by calcium-stimulated adenylyl cyclase activity during fear memory. PLoS One 5:e13385.

Wong ST, Athos J, Figueroa XA, Pineda VV, Schaefer ML, Chavkin CC, Muglia LJ, Storm DR (1999) Calcium-stimulated adenylyl cyclase activity is critical for hippocampus-dependent long-term memory and late phase LTP. Neuron 23:787–798.

Woo NH, Duffy SN, Abel T, Nguyen PV (2003) Temporal spacing of synaptic stimulation critically modulates the dependence of LTP on cyclic AMP-dependent protein kinase. Hippocampus 13:293–300.

Wu ZL, Thomas SA, Villacres EC, Xia Z, Simmons ML, Chavkin C, Palmiter RD, Storm DR (1995) Altered behavior and long-term potentiation in type I adenylyl cyclase mutant mice. Proc Natl Acad Sci U S A 92:220–224.